Journal of Photochemistry & Photobiology, A: Chemistry 451 (2024) 115490

Contents lists available at ScienceDirect

Journal of Photochemistry & Photobiology, A: Chemistry

journal homepage: www.elsevier.com/locate/jphotochem

Improving the sensing ability of thiazolothiazole derivatives towards metal ions

Ana F. R. Cerqueira [a], Nuno M. M. Moura [a], Maria G. P. M. S. Neves [a], A. Jorge Parola [b], Augusto C. Tomé [a,*]

[a] LAQV-REQUIMTE, Department of Chemistry, University of Aveiro, 3810-193 Aveiro, Portugal
[b] LAQV-REQUIMTE, Department of Chemistry, NOVA School of Science and Technology, FCT NOVA, Universidade NOVA de Lisboa, 2829-516 Caparica, Portugal

ARTICLE INFO

Keywords:
Thiazolo[5,4-*d*]thiazole
Chemosensor
Metal ions sensing
Optic sensor
Fluorescent probe

ABSTRACT

Two non-symmetrical thiazolothiazoles (TzTz) incorporating pyridin-2-yl groups were synthesized and their sensing abilities towards a series of metal ions were evaluated. The new compounds exhibited good sensing capabilities towards Cu^{2+} and Zn^{2+}, enabling the differentiation between these two metal ions through spectrophotometric and spectrofluorimetric titrations. The addition of other metal ions to these TzTz derivatives does not cause noticeable effects. The results of this study highlight the high potential of TzTz derivatives for metal ions detection applications.

1. Introduction

The design of new heterocyclic compounds comprising the thiazole scaffold is giving access to molecules with improved features for a variety of applications, namely in the materials chemistry context, due to their strong fluorescence [1], non-linear optical [2] and semiconducting properties [3]. Among them are the thiazolo[5,4-*d*]thiazoles, also known as thiazolothiazoles (TzTz), which are composed by two fused thiazole rings forming a rigid and coplanar structure with an extended π-conjugated system. Due to their photophysical properties and high environmental stability [4–7], TzTz are being successfully explored as components of solar cells devices [8–11], organic light-emitting diodes (OLEDs) [12], luminescent metal–organic frameworks [13], photocatalysts [14,15], and as probes for live-cell imaging [16–18].

Considering the properties of TzTz, the possibility of utilizing them as chemosensors is also deserving attention, but the number of studies exploring this application remains limited. In 2012, Jung and coworkers synthesized TzTz bearing 2-(ethylene oxide)phenyl moieties and evaluated their effectiveness as chemosensors for various metal cations [19]. Some TzTz derivatives exhibited fluorescence enhancement upon addition of Al^{3+} or Cr^{3+}, displaying typical "Off–On" behaviour as fluorescent probes. In general, the modification of TzTz with tertiary aromatic amines resulted in the development of colorimetric and "On–Off" fluorescent TzTz-based chemosensors selective for Cu^{2+} ions [20–22]. However, when the TzTz core was modified with *N,N*-bis(4-methoxyphenyl)aniline moieties, both Cu^{2+} and Fe^{3+} could be detected due to emission quenching upon interaction with both metal ions [23]. Dikmen *et al.* [24] also reported the multi-responsive sensing behavior of 2,5-bis(4-hydroxyphenyl)thiazolo[5,4-*d*]thiazole in the presence of Au^{3+} and Fe^{3+}, resulting in emission quenching due to the formation of TzTz–M^{3+} complexes.

TzTz bearing pyridyl groups display interesting capabilities as luminescent sensors. For instance, the ligand 2,5-di(pyridin-4-yl)thiazolo[5,4-*d*]thiazole was utilized to prepare a MOF with sensing capabilities towards Hg^{2+} [25]. Compared to the pristine MOF, the interaction with Hg^{2+} caused emission quenching accompanied by a red-shift while in the presence of other transition metals, only emission quenching was observed. Also, a fluorescent Zn(II)-MOF based on 2,5-bis[4-(pyridin-4-yl)phenyl]thiazolo[5,4-*d*]thiazole was used as sensor for detecting Al^{3+}, MnO_4^-, CrO_4^{2-}, and $Cr_2O_7^{2-}$ in an aqueous medium [26]. Similarly, a non-symmetrical 2-(pyren-1-yl)-5-(pyridin-4-yl)thiazolo[5,4-*d*]thiazole was recently reported as a "turn-off" emission probe for Hg^{2+} [27].

Although 2,5-di(pyridin-4-yl)TzTz derivatives are frequently used in various applications [16,26–28], 2,5-di(pyridin-2-yl)TzTz derivatives [29–31] have remained almost unexplored, as well as the evaluation of their sensing properties. Interesting examples of the potential of the 2,5-di(pyridin-2-yl)TzTz derivatives for the construction of molecular grids and knots have been reported [32–35]. The scarcity of articles describing the synthesis or transformation of TzTz bearing pyridin-2-yl

* Corresponding author.
E-mail address: actome@ua.pt (A.C. Tomé).

https://doi.org/10.1016/j.jphotochem.2024.115490
Received 21 September 2023; Received in revised form 8 January 2024; Accepted 25 January 2024
Available online 6 February 2024

groups motivated us to modify a 2,5-di(pyridin-2-yl)TzTz derivative aiming to develop new probes with enhanced sensing ability for metal ions.

Among transition metal ions, Cu^{2+} and Zn^{2+} play crucial roles in various biological processes. Thus, the tight control of their levels in the human body is essential, as both deficiency and excess can lead to diseases such as Wilson's, Alzheimer's, or Parkinson's diseases, as well as disorders like hypoxia, ischemia, and epilepsy [36]. Therefore, the development of new chemosensors capable of recognizing these biologically and environmentally relevant metal ions is of great interest.

In this paper, we present the structural modification of a symmetrical 6-methylpyridin-2-ylthiazolothiazole derivative to obtain non-symmetrical derivatives incorporating an additional pyridin-2-yl group. The sensing abilities of both the initial TzTz and the new synthesized derivatives towards a series of metal ions were evaluated through spectrophotometric and spectrofluorimetric titrations aiming to assess how their structural features, namely the presence of an extra pyridine unit or the increased molecular flexibility, influence their sensing capability.

2. Experimental

2.1. Materials and methods

All chemicals were used as provided. Solvents were used as received or dried using standard procedures. ^{1}H and ^{13}C NMR spectra were recorded on Bruker Avance 300 or Bruker Avance 500 spectrometers. $CDCl_3$ was used as solvent and tetramethylsilane (TMS) as internal reference. The chemical shifts are expressed in δ (ppm) and the coupling constants (*J*) in hertz (Hz). The assignment of the signals on the ^{1}H NMR spectra was based on 2D NMR experiments (COSY, HSQC and HMBC). UV–Vis spectra were recorded on a Shimadzu UV-2501PC spectrophotometer using $CHCl_3$ as solvent. The values for λ_{max} are in nm and log ε values were calculated from molar absorptivity in $M^{-1}.cm^{-1}$. Fluorescence emission spectra were recorded with a Horiba FluoroMax 4 spectrofluorometer using $CHCl_3$ as solvent. Fluorescence quantum yields (Φ_F) were determined using 2,5-diphenylthiazolo[5,4-*d*]thiazole as fluorescence standard (Φ_F = 16 %) [37]. Mass spectra were recorded using a Micromass Q-TOF-2™ mass spectrometer and $CHCl_3$ as solvent. High-resolution mass spectra (HRMS-ESI) were obtained in a Q-Exactive® hybrid quadrupole Orbitrap® mass spectrometer (Thermo Fisher Scientific, Bremen, Germany). The instrument was operated in positive mode, with a spray voltage at 3.0 kV and interfaced with a HESI II ion source. The analyses were performed through direct infusion of the prepared solutions at a flow rate of 10 μL min^{-1} into the ESI source. Spectra were analyzed using the acquisition software Xcalibur (ver. 4.0, Thermo Scientific, San Jose, CA, USA). Melting points were determined with a Büchi B-540 melting point apparatus. Preparative thin layer chromatography was carried out on 20 x 20 cm glass plates coated with silica gel (1 mm thick). Analytical TLC was carried out on precoated sheets with silica gel (Merck 60, 0.2 mm thick).

2,5-Bis(6-methylpyridin-2-yl)thiazolo[5,4-*d*]thiazole (**1**) and 2-(6-(bromomethyl)pyridin-2-yl)-5-(6-methylpyridin-2-yl)thiazolo[5,4-*d*]thiazole (**2**) were synthesized using established protocols and their characterization was performed by comparing their ^{1}H NMR spectra with previously reported data [31]. For the spectrophotometric and spectrofluorimetric titrations, stock solutions of **1**, **3** and **4** in chloroform at a concentration of approximately 10^{-3} M were prepared and further diluted to a concentration of 10^{-5} M. Stock solutions of the metal salts [$Cu(OTf)_2$, $ZnCl_2$, AgOTf, $AlCl_3$, $MnCl_2$, $Ni(ClO_4)_2$, KPF_6, $NaBF_4$, $Tl(CF_3COO)_3$, $Cr(acac)_3$, $Pd(acac)_2$, $Cd(OAc)_2$, LiCl] were prepared in acetonitrile at a concentration of 10^{-2} M.

2.2. Synthesis and characterization

2.2.1. Synthesis of (E)-2-(6-methylpyridin-2-yl)-5-[6-(2-(pyridin-2-yl) vinyl)pyridin-2-yl]thiazolo[5,4-d]thiazole (3)

A solution of **2** (35.0 mg, 87.1 μmol) and triphenylphosphine (22.8 mg, 87.1 μmol) in toluene (3 mL) was heated at reflux overnight. After cooling to room temperature, the solvent was removed under reduced pressure and the resulting yellow solid was directly used in the Wittig reaction without further purification. The solid was dissolved in dichloromethane (3 mL), pyridine-2-carbaldehyde (25 μL, 2.6 mmol) and K_2CO_3 (120.3 mg, 871 μmol) were added, and the mixture was stirred at room temperature for 24 h. The reaction mixture was washed with water and the organic compounds were extracted with dichloromethane. The solvent was removed under reduced pressure and the crude was purified by preparative TLC using dichloromethane/hexane (3:1) as the eluent. The expected compound **3** was isolated in 36 % yield (12.9 mg, 31.4 μmol) after crystallization from dichloromethane/methanol.

2.2.2. Synthesis of 2-(6-methylpyridin-2-yl)-5-[6-(2-(pyridin-2-yl)ethyl) pyridin-2-yl]thiazolo[5,4-d]thiazole (4)

To a mixture of **3** (15 mg, 36.3 μmol) and 10 % Pd-C (0.39 mg) in methanol (3 mL) was added, dropwise, triethylsilane (60 μL, 363 μmol, 10 eq.). The reaction mixture was stirred for 2 h under N_2 atmosphere at room temperature. Subsequently, the solution was filtered through celite, and the solvent was evaporated under reduced pressure. The resulting crude mixture was purified by preparative TLC using dichloromethane/hexane (3:1) as the eluent. Crystallization from dichloromethane/methanol afforded TzTz **4** in 66 % yield (9.9 mg, 23.8 μmol).

3. Results and discussion

3.1. Synthesis

The synthetic strategy to prepare TzTz derivatives **3** and **4** is outlined in Scheme 1. The starting 2,5-bis(6-methylpyridin-2-yl)thiazolo[5,4-*d*]thiazole (**1**) was synthesized using a variation of a previously reported procedure [31]. In this case, the condensation reaction between 6-methylpyridine-2-carbaldehyde and dithiooxamide was carried out in DMF at 130 °C for 6 h, resulting in a yield of 83 % for compound **1**. Comparing to the method previously described [31], changing the solvent from $PhNO_2$ to DMF significantly reduced the reaction time (from 24 to 6 h) and increased the yield (from 75 % to 83 %).

The synthesis of compound **3** followed a similar pathway as our previous work on non-symmetrical thiazolo[5,4-*d*]thiazoles bearing styrylpyridyl or hetarylvinylpyridyl groups [31]. Initially, compound **1** was converted into the bromomethyl derivative **2** which was then used to generate the corresponding phosphorus ylide. The *in situ* generated phosphorus ylide underwent a Wittig reaction with pyridine-2-carbaldehyde in the presence of K_2CO_3, at room temperature, affording the expected compound **3** in 36 % yield. The structure of compound **3** was unambiguously confirmed through NMR and mass spectra analysis (see SI). The ^{1}HNMR spectrum (see SI, Fig. S1) exhibited the expected signals for the pyridyl and methyl protons (singlet at 2.64 ppm). The resonances of the two vinylic protons were assigned to the two doublets at δ = 7.71 and 7.85 ppm with J = 15.8 Hz; this large proton–proton coupling constant is a clear indication that the double bond has a *trans* configuration. The mass spectrum displayed the expected peak corresponding to the $[M + H]^+$ ion at m/z = 414 (see Figures S6 and S7).

Compound **4** was prepared via the palladium-promoted hydrogenation of the vinylic double bond of TzTz **3**. The reaction was carried out in MeOH at room temperature, using an excess of triethylsilane (TES) and 10 % Pd-C under N_2 atmosphere [38]. After 2 h, the TLC control confirmed complete conversion of the starting material and the formation of a new compound. After work-up and purification through

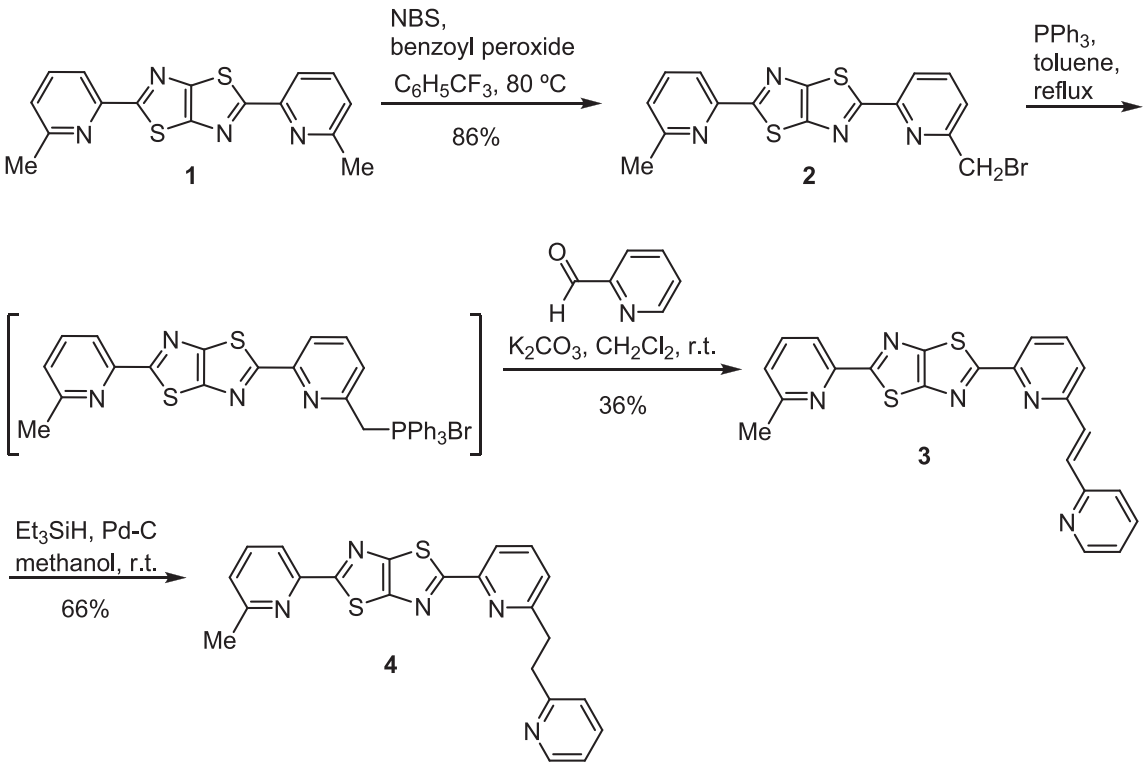

Scheme 1. Synthetic route to TzTz derivatives **3** and **4**.

preparative TLC, compound **4** was obtained in 66 % yield. The structure of compound **4** was confirmed by NMR spectroscopy and mass spectrometry analysis (see SI, Figs. S8–S14).

The ^{1}H NMR spectrum of compound **4** exhibited a new signal in the aliphatic region (slightly broad singlet at δ = 3.37 ppm) corresponding to the resonances of the four protons of the –CH_2–CH_2– chain. The appearance of these four protons at the same chemical shift can be justified by the similarity of their electronic environment. Additionally, the absence of the characteristic doublets of the vinylic protons observed in the spectrum of compound **3** is another evidence of the success of the hydrogenation reaction (see Fig. S8). Also, the ^{13}C NMR spectrum displayed a signal at δ 37.0 ppm, attributed to the resonances of the sp^3 carbons, consistent with the proposed structure (see SI, Fig. S9). This assignment was confirmed by the HSQC spectrum and is in line with the similar electronic environment already pointed out for the four protons of the –CH_2–CH_2– chain (see SI, Fig. S11). The mass spectrum exhibited a peak with m/z = 416 corresponding to the expected $[M + H]^+$ molecular ion (see SI, Figures S13 and S14).

3.2. Photophysical properties

The absorption and emission spectra of TzTz derivatives **1**, **3** and **4**, recorded in chloroform solutions at 298 K, are shown in Fig. 1. Their main spectroscopic and photophysical features are summarized in Table 1. All compounds exhibit a vibrationally resolved lowest energy absorption band with λ_{max} ranging from 366 to 374 nm. The absorption

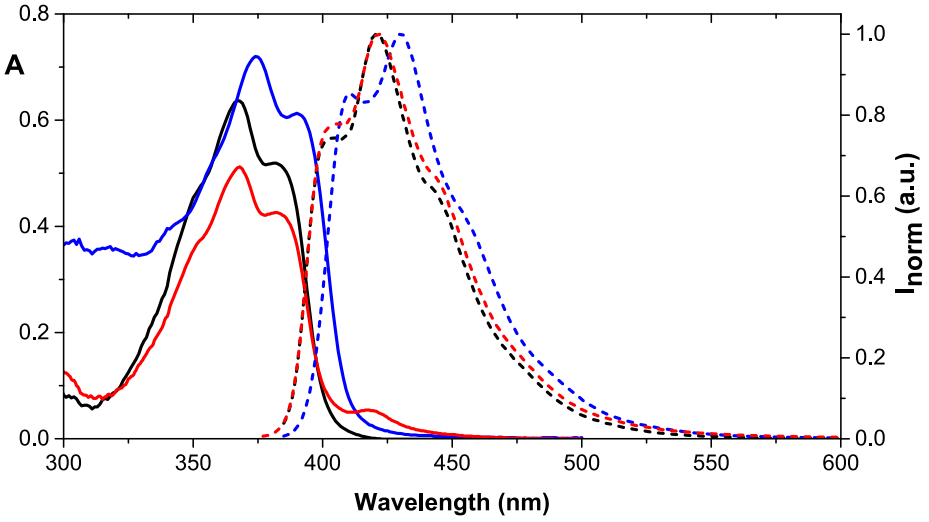

Fig. 1. Absorption (solid lines) and emission (dotted lines) spectra of compounds **1** (black lines), **3** (blue lines) and **4** (red lines) in $CHCl_3$ at 298 K [1] = [3] = [4] = 2×10^{-5} M; λ_{exc1} = 366 nm, λ_{exc3} = 374 nm and λ_{exc4} = 368 nm).

Table 1
Photophysical data of **1**, **3** and **4** in chloroform at 298 K.

Dye	$\lambda_{max,abs}$ (nm)[a]	log ε (M^{-1} cm^{-1})	$\lambda_{max,em}$ (nm)[a]	Stokes shift (cm^{-1})[b]	Φ_F (%)[c]
1	352 sh, 366, 381	4.37, 4.50, 4.41	404, 421, 443 sh	3570	26
3	357 sh, 374, 388	4.41, 4.46, 4.38	411, 429, 458 sh	3427	21
4	352 sh, 368, 383, 419	4.20, 4.33, 4.24, 3.31	400, 422, 446 sh	3477	12

[a] 10^{-5} mol.L^{-1} in $CHCl_3$.
[b] Stokes shift calculated as the difference between the maximum of the first absorption band and the maximum of the fluorescence spectrum [39].
[c] Excitation at 350 nm; calculated using 2,5-diphenylthiazolo[5,4-*d*]thiazole (Φ_F = 16 % in $CHCl_3$) [37] as fluorescence standard.

band of compound **3** is red-shifted by 8 nm relatively to those of compounds **1** and **4**, as a result of the extended π-conjugation, and this pattern is consistent with previous reports [31]. As expected, due to the hydrogenation of the double bond, the UV–Vis spectra of compounds **1** and **4** are very similar (λ_{max} = 366 nm for **1** and 368 nm for **4**). The emission and absorption spectra of all derivatives exhibit the expected mirror symmetry relationship. All compounds show a maximum emission wavelength centered between 421 and 429 nm. The emission spectra of all derivatives also display vibrational resolution. TzTz derivatives **1**, **3** and **4** exhibit Stokes shifts in the range 3427–3570 cm^{-1}, consistent with data reported in the literature [34,35].

The fluorescence quantum yields (Φ_F) were calculated by the internal reference method using 2,5-diphenylthiazolo[5,4-*d*]thiazole as the reference (Φ_F = 16 %) [37]. It was observed that the presence of the pending pyridylvinyl moiety led to a slight decrease in Φ_F from 26 % (for **1**) to 21 % (for **3**), probably due to a reduction in the molecule's rigidity and planarity induced by the pyridylvinyl moiety. This effect is more evident in compound **4** (Φ_F = 12 %) due to the flexible alkyl spacer.

3.3. Spectrophotometric and spectrofluorimetric titrations and metal-sensing effects

The primary objective of this study was to assess the influence of modifications in the TzTz moiety, namely the introduction of an additional binding motif and the reduction of molecular rigidity, on the sensing activity. The sensing capabilities of TzTz derivatives **1**, **3** and **4** towards various metal ions (Al^{3+}, Cr^{3+}, Tl^{3+}, Cd^{2+}, Pd^{2+}, Cu^{2+}, Zn^{2+}, Mn^{2+}, Ni^{2+}, Ag^{+}, Li^{+}, Na^{+} and K^{+}) were investigated by adding small

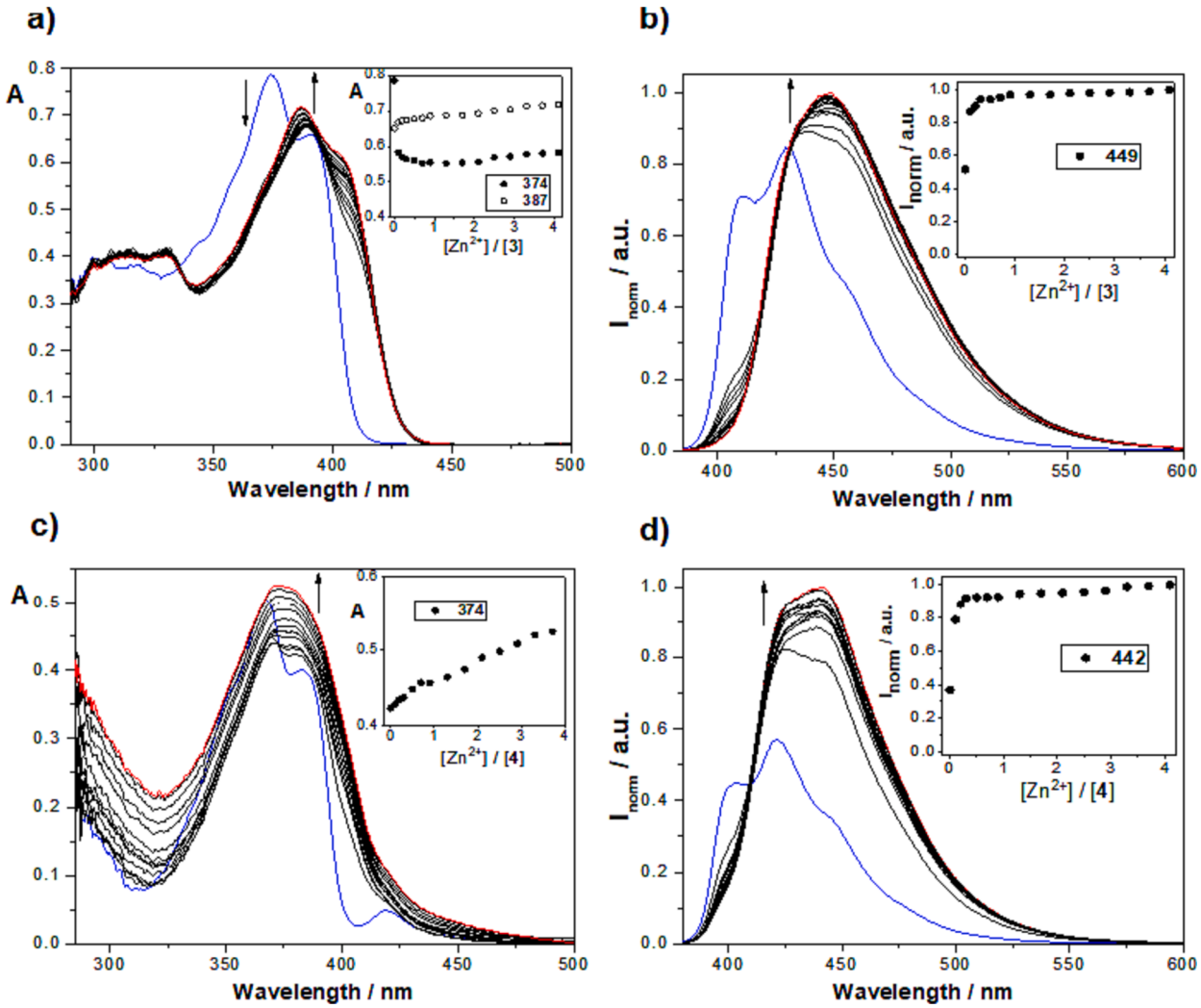

Fig. 2. Spectrophotometric (a and c) and spectrofluorimetric (b and d) titrations of compounds **3** [a) and b)] and **4** [c) and d)] in chloroform as a function of added Zn^{2+} in acetonitrile (initial and final spectra in blue and red, respectively, intermediate spectra in black). The insets show the absorption at 374 and 387 nm (a) and at 374 nm (c); and the normalized emission at 449 nm (b) and 442 nm (d) ([3] = [4] = 2 × 10^{-5} M, λ_{exc3} = 374 nm, λ_{exc4} = 368 nm).

amounts of appropriate metal salts dissolved in acetonitrile to solutions of the ligands dissolved in chloroform. The titrations were followed by absorption and fluorescence emission spectroscopy at 298 K. In general, the titrations of the TzTz derivatives **1**, **3** and **4** with some metal ions resulted in significant changes in both absorption and emission spectra. The most significant interactions were observed upon the addition of Zn^{2+} and Cu^{2+} (Figs. 2–5 and Figs. S9–S16). No noticeable changes were observed when the TzTz derivatives were titrated with Tl^{3+}, Cr^{3+}, Cd^{2+}, Pd^{2+} and Na^{+} ions.

3.3.1. Titration with Zn^{2+}

The sensing ability of the TzTz derivatives **1**, **3** and **4** towards Zn^{2+} was accessed through spectrophotometric and spectrofluorimetric titrations with an acetonitrile solution of $ZnCl_2$. The addition of aliquots of the Zn(II) solution to $CHCl_3$ solutions of TzTz **1**, **3**, and **4** induced substantial changes in absorption and emission spectra, as depicted in Fig. 2 for TzTz derivatives **3** and **4** and in Fig. S15 for TzTz derivative **1**.

The spectrophotometric titration of ligand **3** with Zn^{2+} resulted in a red-shift of 13 nm in the UV–Vis spectrum, indicating the formation of the **3**–Zn^{2+} complex (Fig. 2a). A similar red-shift of 13 nm along with a slight decrease in intensity (hypochromism) was observed for the complex **1**–Zn^{2+} (Fig. S15a). On the other hand, the titration of the hydrogenated TzTz derivative **4** with Zn^{2+} displayed different changes when compared to those described for compounds **1** and **3** (Fig. 2c). In this case, the bathochromic shift was smaller (6 nm) and was accompanied by the formation of a single and broader absorption band centered at 374 nm; this new band, attributed to the **4**–Zn^{2+} complex, exhibited a slight increase in intensity (hyperchromism) when compared to the free molecular probe **4**.

In terms of emission spectra, all three TzTz derivatives showed a strong ratiometric response in the presence of Zn^{2+} (Fig. 2b,d and Fig. S15b). Upon titration, the initial emission bands gradually shift to the red while increasing in intensity and decreasing vibrational resolution, attributed to the formation of the ligand–Zn^{2+} complexes. The maximum wavelength of the complexes ranged from 442 (for **1** and **4**) to 449 nm (for **3**).

Furthermore, the modifications performed at the TzTz core significantly enhanced the sensing ability of the studied compounds for Zn^{2+} detection. While TzTz derivative **1** required the addition of approximately 7 equivalents of the metal ion to reach a plateau corresponding to the TzTz–metal complex, compounds **3** and **4** only required around 3 equivalents of the metal ion to attain a plateau.

To ensure that the observed changes were indeed due to ligand–metal interactions and not ligand–anion binding, titrations of TzTz derivatives **1** and **3** with tetrabutylammonium (TBA) chloride were conducted under the same conditions. No changes were observed in absorption or emission spectra upon addition of TBA chloride (Fig. S16). Similarly, to confirm that the observed spectral changes were not caused by *in situ* generation of HCl (via $CHCl_3$) and subsequent protonation of the pyridine moieties, spectrophotometric and spectrofluorimetric titrations of compounds **1** and **3** with HCl were performed. Once again, no significant changes were observed for compound **1** during these titrations nor for compound **3** during the spectrophotometric titrations. In these assays, the main alterations were observed in the spectrofluorimetric titration of TzTz **3**, with just a decrease in intensity of the emission bands at 411 and 429 nm (Fig. S17). These two experiments confirmed that the alterations observed in the absorption and emission spectra upon addition of $ZnCl_2$ were solely due to metal–ligand interactions.

3.3.2. Titration with Cu^{2+}

The sensing capability of compounds **1**, **3** and **4** towards Cu^{2+} ions was evaluated, by performing titrations with a solution of $Cu(OTf)_2$ in acetonitrile. The addition of Cu^{2+} to $CHCl_3$ solutions of **1**, **3** and **4** resulted in significant changes in their absorption and emission spectra (Figures 3 and S18). In general, all the ligands showed "On-Off" fluoroionophoric behavior, losing their fluorescence ability upon binding to Cu^{2+} ions.

During these titrations, the alterations observed in the absorption spectra for compounds **1** and **3** with Cu^{2+} were similar. The initial absorption band decreased in intensity, and a new band emerged with a maximum at 414 nm for compound **1** and 427 nm for compound **3** (Figs. S18a and 3a, respectively). For compound **1**, the presence of an isosbestic point at 394 nm suggested the coexistence of only two species in solution, corresponding to the free ligand and the mononuclear metal complex. In the case of compound **4**, the absorption spectrum exhibited a 7 nm red-shift along with an increase in intensity of a new absorption band at 375 nm. This new band can be attributed to the interaction between the ligand and the metal ion, indicating the formation of the corresponding metal complexes (Fig. S18c).

The spectrofluorimetric titrations of compounds **1**, **3** and **4** with Cu^{2+} exhibited significant emission quenching, with an almost complete suppression: >99 % for **1** and **3** and approximately 95 % for compound **4** (Fig. 3b and S18b,d). This quenching behavior can be attributed to

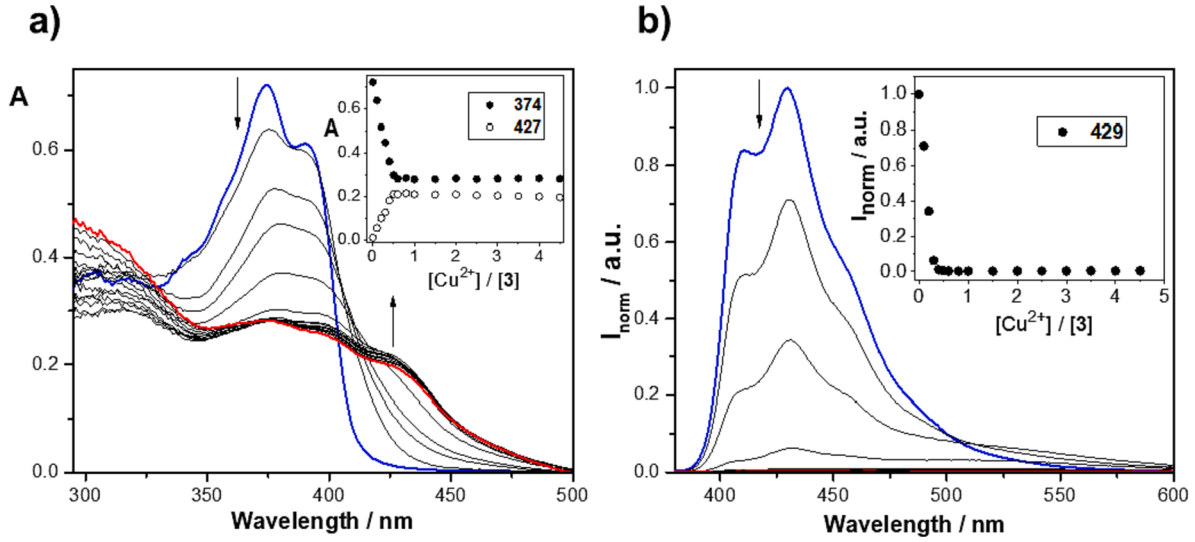

Fig. 3. Spectrophotometric (a) and spectrofluorimetric (b) titrations of compound **3** in chloroform as a function of added Cu^{2+} in acetonitrile (initial and final spectra in blue and red, respectively, intermediate spectra in black). The insets show the absorption at 374 and 427 nm (a); and the normalized emission at 429 nm (b) ([**3**] = 2×10^{-5} M, $\lambda_{exc3} = 374$ nm).

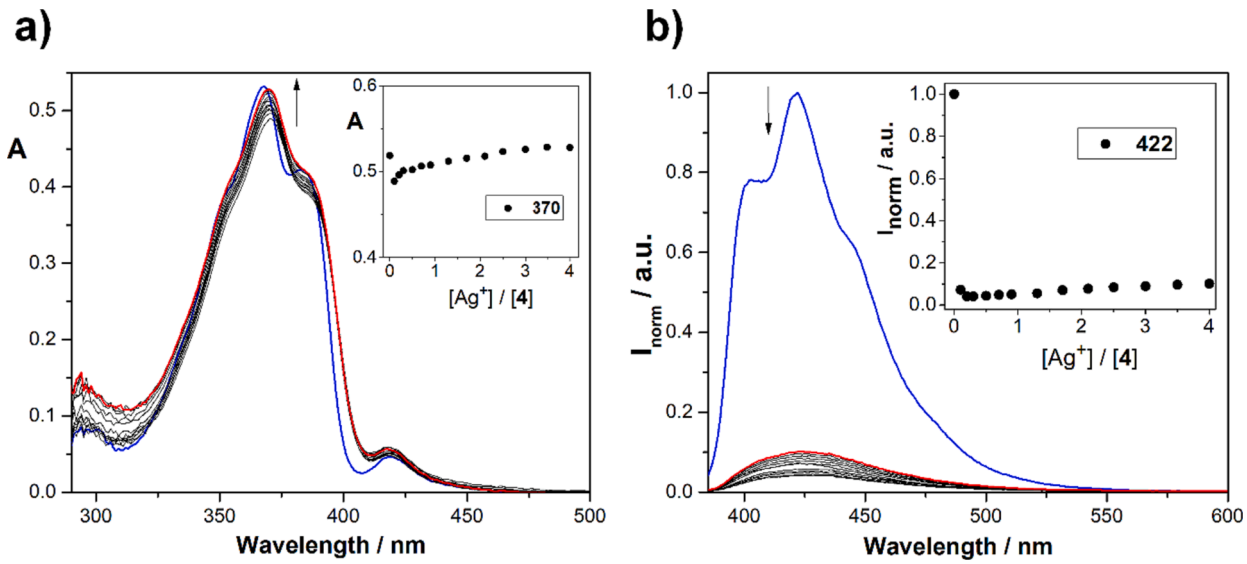

Fig. 4. Spectrophotometric (a) and spectrofluorimetric (b) titrations of compound **4** in chloroform as a function of added Ag^{+} in acetonitrile (initial and final spectra in blue and red, respectively, intermediate spectra in black). The insets show the absorption at 370 nm (a); and the normalized emission at 422 nm (b) ([4] = 2×10^{-5} M, λ_{exc} = 368 nm).

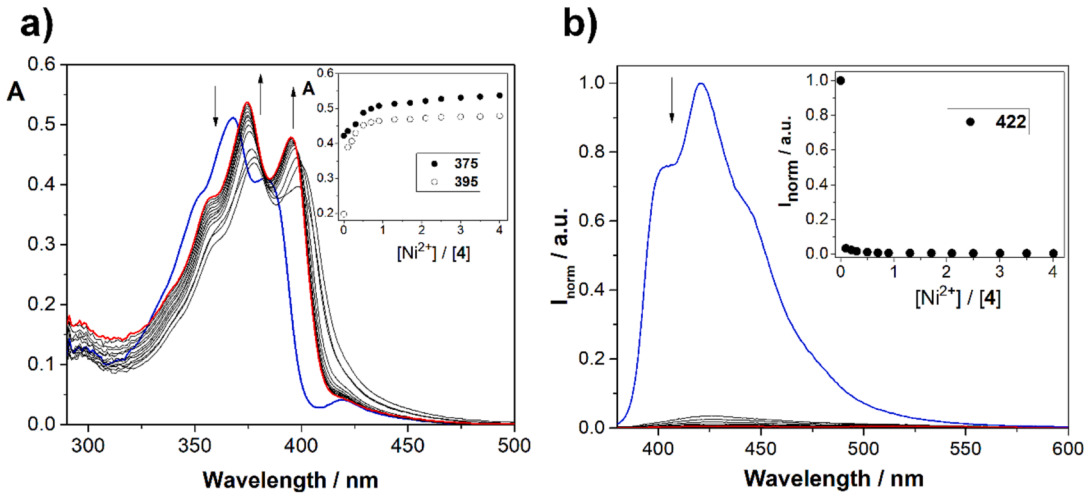

Fig. 5. Spectrophotometric (a) and spectrofluorimetric (b) titrations of compound **4** in chloroform as a function of added Ni^{2+} in acetonitrile (initial and final spectra in blue and red, respectively, intermediate spectra in black). The insets show the absorption at 375 and 395 nm (a); and the normalized emission at 422 nm (b) ([4] = 2×10^{-5} M, λ_{exc} = 368 nm).

nonradiative deactivation processes, which can occur through various pathways, such as the formation of the excited triplet state via electron spin–orbit coupling induced by the heavy metal effect of Cu^{2+} or reversible electron transfer. The quenching effect was slightly more pronounced for derivatives **1** and **3** than for **4**, although the first two TzTz derivatives required a higher amount of the metal ion to reach the plateau. For compounds **1** and **3,** the plateau was reached after the addition of 3.5 and 1 equivalents, respectively, whereas for compound **4** only 0.5 equivalents of Cu^{2+} were required. These results further support the enhancements achieved by reducing the double bond, which imparts lower molecular rigidity, enabling stabilization of the ligand–metal complex.

3.3.3. *Titration with Ag^{+}*

The alterations observed during the titrations of the TzTz probes with the Ag^{+} salt were more evident in the emission than in the absorption spectra (Figures 4 and S19). All UV–Vis spectra exhibited bathochromic absorption shifts upon coordination with Ag^{+}, but these are relatively small when compared to those observed upon interaction with Zn^{2+} and Cu^{2+}. The parent scaffold TzTz **1** displayed a red-shift of 1 nm, while compounds **3** and **4** showed a 2 nm red-shift along with the red-shift of the shoulder band to 393 and 386 nm, respectively (Fig. 4a and S19a,c). Concerning the spectrofluorimetric titrations, coordination to Ag^{+} ions resulted in emission quenching for all TzTz derivatives, with varying degrees of effectiveness. The quenching effect was less pronounced for TzTz derivatives **1** (≈ 45 %) and **3** (≈ 65 %) but quite significant for **4** (≈ 90 %) (Fig. 4b and Fig. S19b,d). The heavy atom effect of silver and formation of aggregates due to the interaction of the TzTz with Ag^{+} can also contribute to the observed fluorescence quenching [40].

3.3.4. *Titration with other metal ions*

The chemosensing properties of the TzTz probes towards other metal ions were also investigated under identical experimental conditions (Table 2). Surprisingly, while TzTz **1** exhibited interactions with Ni^{2+} and Mn^{2+} that resulted in changes in both UV–Vis and emission spectra

Table 2
Stability constants for TzTz chemosensors **1**, **3** and **4** in the presence of metal ions in $CHCl_3$ and stoichiometry for the ligand–metal (L:M) interaction at 298 K.

Compound	Metal	Σ log K (abs)	Σ log K (emiss)	Interaction (L:M)
1	Zn^{2+}	$1.52 \pm 2.0 \times 10^{-3}$	1.34 ± 0.01	2:1
	Cu^{2+}	$1.48 \pm 1.0 \times 10^{-3}$	1.68 ± 0.01	2:1
	Ag^{+}	$1.17 \pm 3.9 \times 10^{-3}$	1.02 ± 0.04	1:1
	Ni^{2+}	$1.64 \pm 1.0 \times 10^{-3}$	1.60 ± 0.02	2:1
	Mn^{2+}	$1.64 \pm 7.3 \times 10^{-3}$	1.52 ± 0.03	2:1
	Al^{3+}	$0.96 \pm 1.0 \times 10^{-3}$	0.94 ± 0.01	3:1
	K^{+}	$0.72 \pm 1.9 \times 10^{-3}$	–	1:1
	Li^{+}	–	–	–
	Na^{+}	–	–	–
	Pd^{2+}	–	–	–
	Cd^{2+}	–	–	–
	Tl^{3+}	–	–	–
	Cr^{3+}	–	–	–
3	Zn^{2+}	$5.23 \pm 2.4 \times 10^{-3}$	4.97 ± 0.01	1:1
	Cu^{2+}	$4.94 \pm 1.0 \times 10^{-3}$	4.93 ± 0.01	1:1
	Ag^{+}	$3.60 \pm 4.0 \times 10^{-3}$	3.40 ± 0.01	1:1
	Ni^{2+}	–	–	–
	Mn^{2+}	–	–	–
	Al^{3+}	$2.70 \pm 2.1 \times 10^{-3}$	2.84 ± 0.01	1:1
	K^{+}	–	–	–
	Li^{+}	–	4.24 ± 0.01	1:1
	Na^{+}	–	–	–
	Pd^{2+}	–	–	–
	Cd^{2+}	–	–	–
	Tl^{3+}	–	–	–
	Cr^{3+}	–	–	–
4	Zn^{2+}	$4.50 \pm 1.5 \times 10^{-3}$	4.33 ± 0.01	1:1
	Cu^{2+}	$6.11 \pm 1.2 \times 10^{-3}$	5.94 ± 0.01	1:1
	Ag^{+}	$6.65 \pm 2.6 \times 10^{-3}$	6.45 ± 0.03	1:1
	Ni^{2+}	$4.73 \pm 2.6 \times 10^{-3}$	4.56 ± 0.03	1:1
	Mn^{2+}	–	–	–
	Al^{3+}	–	–	–
	K^{+}			
	Li^{+}	$3.63 \pm 5.9 \times 10^{-3}$	4.16 ± 0.01	1:1
	Na^{+}	–	–	–
	Pd^{2+}	–	–	–
	Cd^{2+}	–	–	–
	Tl^{3+}	–	–	–
	Cr^{3+}	–	–	–

(Fig. S20), compounds **3** and **4** did not show any noticeable changes. The addition of Ni^{2+} to a solution of probe **1** induced similar changes to those observed with Zn^{2+}, but it required the addition of over 20 equivalents of Ni^{2+} to reach the ligand–metal complex stabilization (Fig. S20a). In the spectrophotometric titration of **1** with Mn^{2+}, hypochromic and hyperchromic effects were observed for the bands at 366 nm and 381 nm, respectively, without a significant bathochromic effect (Fig. S20c).

Concerning the spectrofluorimetric titrations, ligand **1** exhibited different behaviors in the presence of Ni^{2+} and Mn^{2+} (Figs. S20b,d). Initially, the addition of Ni^{2+}, led to an increase in the emission band at 441 nm, followed by pronounced quenching (≈ 80 %). On the other hand, the interaction of **1** with Mn^{2+} resulted in emission enhancement and the formation of a new emission band at 440 nm, corresponding to the formation of the **1**–Mn^{2+} complex. Ligands **3** and **4** did not exhibit any changes, both in absorption or emission, during titration with Mn^{2+}. However, in the presence of Ni^{2+}, TzTz **3** and **4** displayed different behaviors. Ligand **3** did not interact with metal cation, even after the addition of an excess of the appropriate salt. In contrast, ligand **4** showed changes in both titrations. The absorption titration revealed the formation of two new absorption bands at 375 and 395 nm due to the formation of the **4**–Ni^{2+} complex. In the spectrofluorimetric titration, a rapid and complete emission quenching was observed (Fig. 5).

Concerning the titrations with the trivalent metal ions Al^{3+}, Tl^{3+} and Cr^{3+}, significant changes were observed only for TzTz derivatives **1** and **3** in the presence of Al^{3+}. In both cases, a slight bathochromic shift of the initial absorption band was observed due to the formation of the corresponding ligand–Al^{3+} complexes. The addition of Al^{3+} to TzTz **1** and **3** resulted in a 40 % and 20 % decrease in emission, respectively (Fig. S21).

In the case of titrations with monovalent cations (Li^{+} and K^{+}), TzTz **1** exhibited interaction capability only with K^{+}, while compounds **3** and **4** showed changes only in the presence of Li^{+}. The addition of K^{+} to **1** induced changes solely in the absorption spectrum, with a slight hyperchromic effect observed for the bands centered at 366 and 381 nm due to the formation of the **1**–K^{+} complex (Fig. 6a). No noticeable changes were observed in the emission spectrum of TzTz **1** upon the addition of K^{+}.

For TzTz derivatives **3** and **4**, the addition of Li^{+} resulted in two distinct behaviors. In the case of compound **3**, the addition of Li^{+} did not induce changes in the absorption spectrum (Fig. S22a), while for TzTz **4** there was a clearer increase in the intensity of the absorption bands (≈ 50 %) (Fig. S22c). In the emission titration, a slight quenching of the two initial emission bands was observed for both ligands **3** and **4** (Fig. S22b, d).

The stability constants for the interaction of compounds **1**, **3** and **4** with the metal ions were determined using HypSpec software. The results of these calculations are summarized in Table 2.

The stability constants determined for TzTz **1** were found to be ranging from 1.64 to 0.72. These low values confirm its limited metal ion binding ability and poor selectivity. Additionally, large amounts of each metal ion were required to stabilize the ligand **1**–metal complexes, which may be attributed to the absence of additional binding motifs in **1**. The binding modes between the ligand and metal ions indicate that the stoichiometry of the complex formed depends on the charge of the metal ion. For TzTz **1**, the ligand–metal complexes (L:M) exhibited stoichiometries of 1:1, 2:1, or 3:1 with mono-, di-, or trivalent metal ions, respectively.

The structural modifications performed at the TzTz core by introducing of a styrylpyridyl unit and its reduced counterpart (TzTz derivatives **3** and **4**, respectively) significantly enhanced the sensing activity of both derivatives compared to the precursor **1**. This improvement can be attributed to the additional pyridine binding motif. In both cases, the results of the metal ion titrations suggest the formation of complexes with a L:M ratio of 1:1. The presence of the additional pyridine unit allowed a significant reduction of the amount of metal ion required to stabilize the complex and greatly improved the sensing ability and selectivity of the TzTz probes. This improvement is likely due to the formation of a binding cavity suitable for coordinating metal ions with a radius of approximately 70 to 80 pm. This can explain the demonstrated sensing ability of TzTz probes **3** and **4** towards Li^{+}, while TzTz **1** is capable of binding K^{+}. Stability constants ranging from $\Sigma\log\beta = 2.70$ to $\Sigma\log\beta = 5.23$ were obtained for TzTz **3**, while the reduction of the vinyl bridge further improved the selectivity and led to stability constants ranging from $\Sigma\log\beta = 3.63$ to $\Sigma\log\beta = 6.65$ for TzTz **4**. These data highlight the importance of the saturated bridge, which enhances molecular flexibility and facilitates the formation of more stable ligand–metal complexes. The obtained results for both probes **3** and **4** support a 1:1 ligand-to-metal stoichiometry.

Furthermore, macroscopic changes were observed when 1 equivalent of Zn^{2+} was added to both compounds **3** and **4** under UV excitation at 365 nm (Fig. 7). The interaction of these ligands with Zn^{2+} resulted in an intense light blue emission. As expected, full emission quenching was observed for both ligands in the presence of Cu^{2+}, while compound **4** exhibited a similar behavior in the presence of Ag^{+} and Ni^{2+}. No changes in emission were observed when 1 equivalent of the remaining metal cations was added to the solutions of ligands **3** and **4**, compared to the initial emission of each ligand in $CHCl_3$.

The structural modifications described in this study successfully improved the selectivity of the new ligands compared to the original ligand **1**. In fact, TzTz derivatives **3** and **4** exhibited promising sensing capabilities specifically towards Cu^{2+} and Zn^{2+}, enabling the

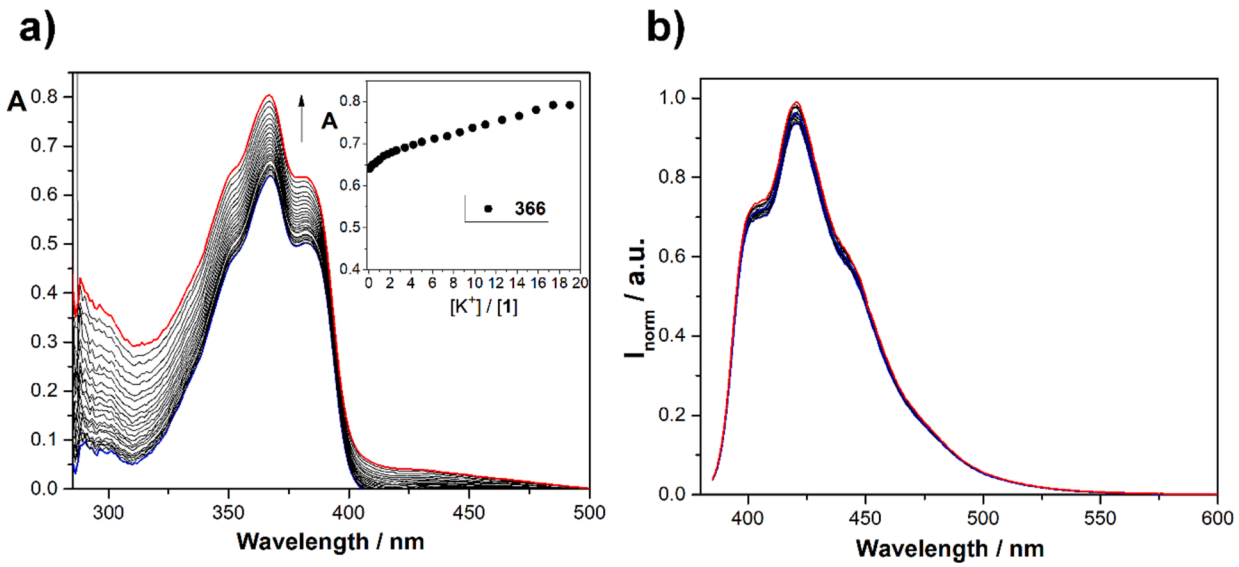

Fig. 6. Spectrophotometric (a) and spectrofluorimetric (b) titrations of TzTz **1** in chloroform as a function of added K^+ in acetonitrile (initial and final spectra in blue and red, respectively, intermediate spectra in black). The insets show the absorption at 366 nm ([1] = 2 × 10^{-5} M, λ_{exc} = 366 nm).

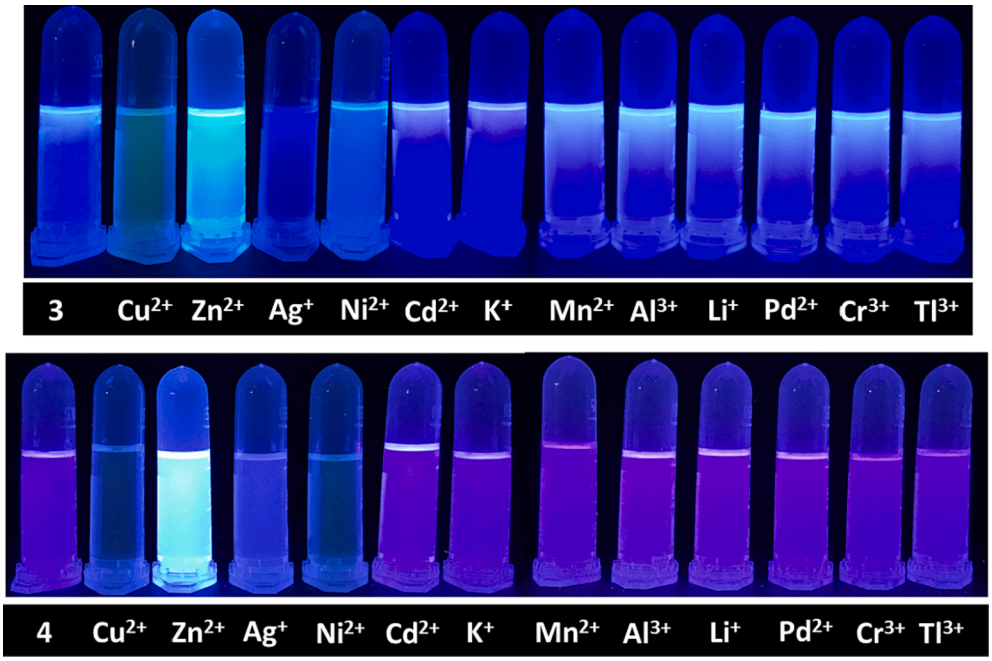

Fig. 7. Observed changes in the physical appearance of solutions of compounds **3** (top) and **4** (bottom) in $CHCl_3$ upon the addition of 1.0 equivalent of various metal ions in CH_3CN under UV light (λ = 365 nm).

differentiation between these two metal ions. Fig. 8 illustrates the absorption response of compounds **3** and **4** towards selected metal cations, revealing selectivity in the interaction between TzTz derivative **3** with Cu^{2+}, being observed a significant absorption decrease of over 55 % at 374 and 387 nm. Fluorescence analysis revealed that the interaction of compound **3** with Cu^{2+} completely quenched the emission, whereas compound **4** exhibited a strong increase in the emission band at 441 nm in the presence of Zn^{2+}. These findings show that TzTz derivatives **3** and **4** can be used for the selective detection of Cu^{2+} and Zn^{2+} using absorption and/or emission spectroscopies.

4. Conclusions

In summary, the functionalization of TzTz **1** with an additional pyridine unit afforded two novel chemosensors for metal ions. The results discussed above confirm that the addition of a flexible pendent pyridin-2-yl group to the starting TzTz **1** greatly improved the sensing ability of the resulting TzTz derivatives **3** and **4** towards Cu^{2+} and Zn^{2+}. While the interaction between TzTz **3** with Cu^{2+} resulted in a significant absorption decrease at 374 and 387 nm, and a complete quench of the emission, TzTz **4** exhibited a strong increase in the emission band at 441 nm in the presence of Zn^{2+}. Additionally, the obtained results indicated a 1:1 ligand-to-metal complex stoichiometry for both TzTz **3** and **4**. It is also worth highlighting that the presence of the extra pyridine unit allowed a significant decrease in the amount of metal ions required to stabilize the complexes. These findings highlight the high potential of these TzTz derivatives for the determination of zinc and copper species based on the absorption and fluorescence signals.

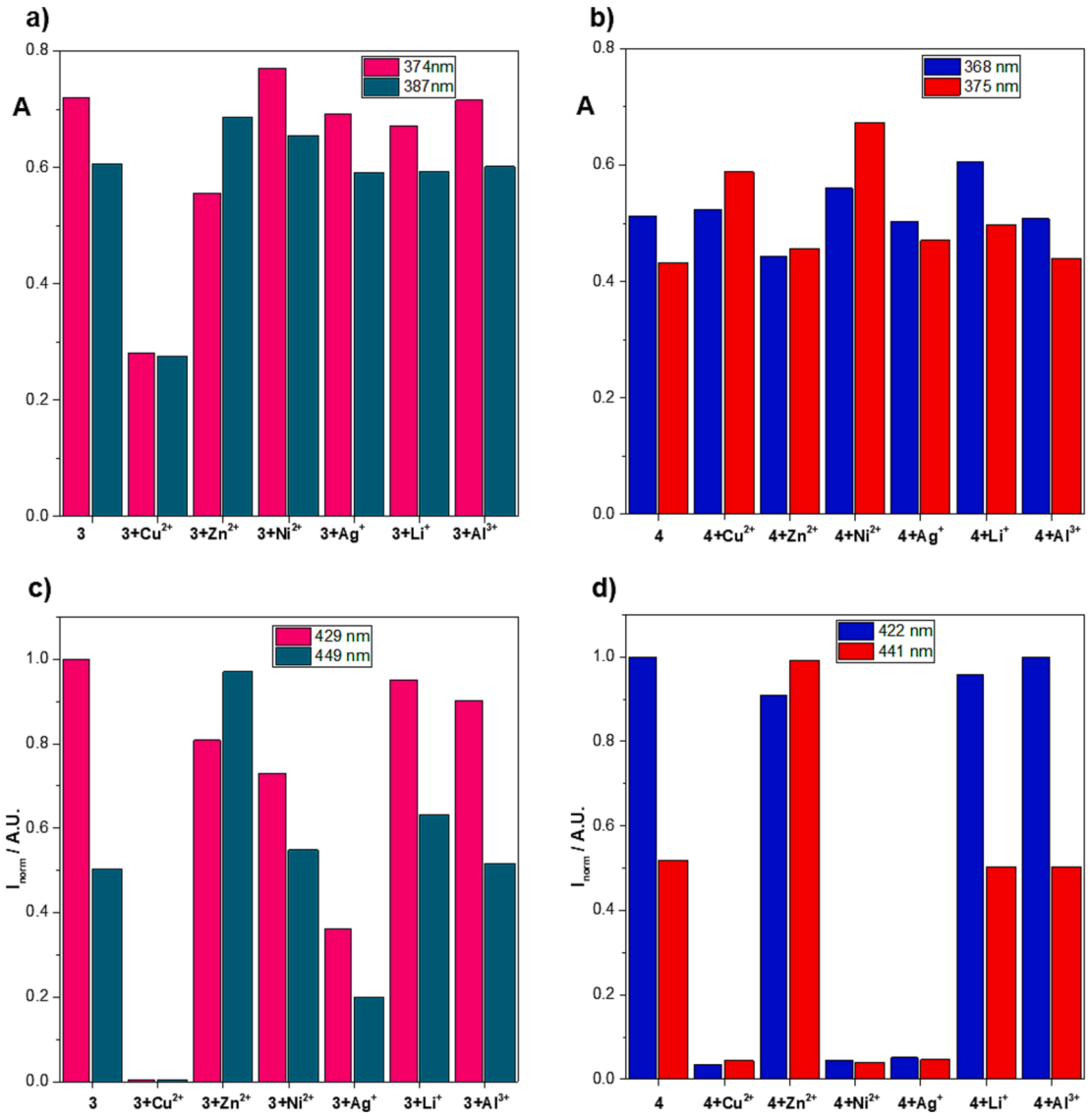

Fig. 8. Comparative absorption and fluorescence response of probes **3** [a) and c)] and **4** [b) and d)] to Cu^{2+}, Zn^{2+}, Ni^{2+}, Ag^{+}, Li^{+} and Al^{3+} (1 equiv.) in chloroform ([3] = [4] = 2×10^{-5} M; λ_{exc3} = 374 nm; λ_{exc4} = 368 nm).

Funding

This work received financial support from PT national funds (FCT/MCTES, Fundação para a Ciência e a Tecnologia and Ministério da Ciência, Tecnologia e Ensino Superior) for LAQV-REQUIMTE through the projects UIDB/50006/2020 and UIDP/50006/2020. N. Moura thanks FCT for funding through program DL 57/2016 – Norma transitória (REF.-048-88-ARH/2018).

Declaration: The authors declare that no generative artificial intelligence (AI) and AI-assisted technologies were used in the writing of this article.

CRediT authorship contribution statement

Ana F. R. Cerqueira: Investigation, Writing – original draft, Data curation. **Nuno M. M. Moura:** Investigation, Writing – original draft, Data curation. **Maria G. P. M. S. Neves:** Supervision, Writing – review & editing. **A. Jorge Parola:** Supervision, Writing – review & editing. **Augusto C. Tomé:** Writing – review & editing, Supervision, Resources, Methodology, Conceptualization.

Declaration of competing interest

The authors declare that they have no known competing financial interests or personal relationships that could have appeared to influence the work reported in this paper.

Data availability

Data will be made available on request.

Acknowledgements

Thanks are due to the University of Aveiro and FCT/MCTES for the financial support through PT national funds for LAQV-REQUIMTE (UIDB/50006/2020 and UIDP/50006/2020), within the PT2020 Partnership Agreement, and to the Portuguese NMR Network. A. Cerqueira thanks FCT/MCTES for her doctoral grant (SFRH/BD/135597/2018). N. Moura thanks FCT for funding through program DL 57/2016 – Norma transitória (REF.-048-88-ARH/2018).

Appendix A. Supplementary data

Supplementary data to this article can be found online at https://doi.org/10.1016/j.jphotochem.2024.115490.

References

[1] R.M.F. Batista, S.P.G. Costa, M.M.M. Raposo, Synthesis of new fluorescent 2-(2′,2″-bithienyl)-1,3-benzothiazoles, Tetrahedron Lett. 45 (2004) 2825–2828, https://doi.org/10.1016/j.tetlet.2004.02.048.

[2] J. Ren, S.M. Wang, L.F. Wu, Z.X. Xu, B.H. Dong, Synthesis and properties of novel Y-shaped NLO molecules containing thiazole and imidazole chromophores, Dye. Pigment. 76 (2008) 310–314, https://doi.org/10.1016/j.dyepig.2006.09.003.

[3] S. Ando, R. Murakami, J.I. Nishida, H. Tada, Y. Inoue, S. Tokito, Y. Yamashita, n-type organic field-effect transistors with very high electron mobility based on thiazole oligomers with trifluoromethylphenyl groups, J. Am. Chem. Soc. 127 (2005) 14996–14997, https://doi.org/10.1021/ja055686f.

[4] R.C. Knighton, A.J. Hallett, B.M. Kariuki, S.J.A. Pope, A one-step synthesis towards new ligands based on aryl-functionalised thiazolo[5,4-*d*]thiazole chromophores, Tetrahedron Lett. 51 (2010) 5419–5422, https://doi.org/10.1016/j.tetlet.2010.07.172.

[5] G. Reginato, M. Calamante, A. Dessì, A. Mordini, M. Peruzzini, L. Zani, Cross-coupling reactions: some applications to the synthesis of thiazolothiazole- and benzobisthiazole-based dyes for new generation solar cells (DSSC), J. Organomet. Chem. 771 (2014) 117–123, https://doi.org/10.1016/j.jorganchem.2014.01.024.

[6] D. Bevk, L. Marin, L. Lutsen, D. Vanderzande, W. Maes, Thiazolo[5,4-*d*]thiazoles-promising building blocks in the synthesis of semiconductors for plastic electronics, RSC Adv. 3 (2013) 11418–11431, https://doi.org/10.1039/c3ra40851e.

[7] Y. Lin, H. Fan, Y. Li, X. Zhan, Thiazole-based organic semiconductors for organic electronics, Adv. Mater. 24 (2012) 3087–3106, https://doi.org/10.1002/adma.201200721.

[8] G. Reginato, A. Mordini, L. Zani, M. Calamante, A. Dessì, Photoactive compounds based on the thiazolo[5,4-*d*]thiazole core and their application in organic and hybrid photovoltaics, European J. Org. Chem. 2016 (2016) 233–251, https://doi.org/10.1002/ejoc.201501237.

[9] M. Nazim, S. Ameen, M. Shaheer Akhtar, H.S. Shin, D-Π-A-Π-D type thiazolo[5,4-*d*]thiazole-core organic chromophore and graphene modified PEDOT:PSS buffer layer for efficient bulk heterojunction organic solar cells, Sol. Energy. 171 (2018) 366–373, https://doi.org/10.1016/j.solener.2018.06.087.

[10] A. Dessì, M. Calamante, A. Sinicropi, M.L. Parisi, L. Vesce, P. Mariani, B. Taheri, M. Ciocca, A. Di Carlo, L. Zani, A. Mordini, G. Reginato, Thiazolo[5,4-*d*]thiazole-based organic sensitizers with improved spectral properties for application in greenhouse-integrated dye-sensitized solar cells, Sustain Energy Fuels 4 (2020) 2309–2321, https://doi.org/10.1039/d0se00124d.

[11] Y. Wang, Y. Wang, L. Zhu, H. Liu, J. Fang, X. Guo, F. Liu, Z. Tang, M. Zhang, Y. Li, A novel wide-bandgap small molecule donor for high efficiency all-small-molecule organic solar cells with small non-radiative energy losses, Energy Environ. Sci. 13 (2020) 1309–1317, https://doi.org/10.1039/c9ee04199k.

[12] Z. Zhang, Y.A. Chen, W.Y. Hung, W.F. Tang, Y.H. Hsu, C.L. Chen, F.Y. Meng, P. T. Chou, Control of the reversibility of excited-state intramolecular proton transfer (ESIPT) reaction: host-polarity tuning white organic light emitting diode on a new thiazolo[5,4-*d*]thiazole ESIPT system, Chem. Mater. 28 (2016) 8815–8824, https://doi.org/10.1021/acs.chemmater.6b04707.

[13] P. Li, X.-M. Yin, L.-L. Gao, S.-L. Yang, Q. Sui, T. Gong, E.-Q. Gao, Modulating excitation energy of luminescent metal-organic frameworks for detection of Cr(VI) in water, ACS Appl. Nano Mater. 2 (2019) 4646–4654, https://doi.org/10.1021/acsanm.9b01088.

[14] Q. Huang, L. Guo, N. Wang, X. Zhu, S. Jin, B. Tan, Layered thiazolo[5,4-*d*]thiazole-linked conjugated microporous polymers with heteroatom adoption for efficient photocatalysis application, ACS Appl. Mater. Interfaces. 11 (2019) 15861–15868, https://doi.org/10.1021/acsami.8b21765.

[15] Y. Wang, H. Liu, Q. Pan, N. Ding, C. Yang, Z. Zhang, C. Jia, Z. Li, J. Liu, Y. Zhao, Construction of thiazolo[5,4-*d*]thiazole-based two-dimensional network for efficient photocatalytic CO_2 reduction, ACS Appl. Mater. Interfaces. 12 (2020) 46483–46489, https://doi.org/10.1021/acsami.0c12173.

[16] I. Roy, S. Bobbala, J. Zhou, M.T. Nguyen, S.K.M. Nalluri, Y. Wu, D.P. Ferris, E. A. Scott, M.R. Wasielewski, J.F. Stoddart, ExTzBox: a glowing cyclophane for live-cell imaging, J. Am. Chem. Soc. 140 (2018) 7206–7212, https://doi.org/10.1021/jacs.8b03066.

[17] B. Li, X. Lu, Y. Tian, D. Li, Embedding multiphoton active units within metal-organic frameworks for turning on high-order multiphoton excited fluorescence for bioimaging, Angew. Chem. Int. Ed. Engl. 61 (2022) e202206755.

[18] N.A. Sayresmith, A. Saminathan, J.K. Sailer, S.M. Patberg, K. Sandor, Y. Krishnan, M.G. Walter, Photostable voltage-sensitive dyes based on simple, solvatofluorochromic, asymmetric thiazolothiazoles, J. Am. Chem. Soc. 141 (2019) 18780–18790, https://doi.org/10.1021/jacs.9b08959.

[19] J.Y. Jung, S.J. Han, J. Chun, C. Lee, J. Yoon, New thiazolothiazole derivatives as fluorescent chemosensors for Cr^{3+} and Al^{3+}, Dye. Pigment. 94 (2012) 423–426, https://doi.org/10.1016/j.dyepig.2012.02.005.

[20] J.Y. Jung, M. Kang, J. Chun, J. Lee, J. Kim, J. Kim, Y. Kim, S.J. Kim, C. Lee, J. Yoon, A thiazolothiazole based Cu^{2+} selective colorimetric and fluorescent sensor via unique radical formation, Chem. Commun. 49 (2013) 176–178, https://doi.org/10.1039/c2cc36626f.

[21] X. Zhang, M. Kang, H.A. Choi, J.Y. Jung, K.M.K. Swamy, S. Kim, D. Kim, J. Kim, C. Lee, J. Yoon, Organic radical-induced Cu^{2+} selective sensing based on thiazolothiazole derivatives, Sensors Actuators, B Chem. 192 (2014) 691–696, https://doi.org/10.1016/j.snb.2013.11.027.

[22] X. Zhang, H.A. Choi, S. Lee, J. Yin, S.H. Kim, C. Lee, J. Yoon, A cholesteryl thiazolothiazole derivative for colorimetric sensing of Cu^{2+} and its sol–gel transition, Dye. Pigment. 122 (2015) 109–115, https://doi.org/10.1016/J.DYEPIG.2015.06.016.

[23] G. Sathiyan, S. Chatterjee, P. Sen, A. Garg, R.K. Gupta, A. Singh, Thiazolothiazole-based fluorescence probe towards detection of copper and iron ions through formation of radical cations, ChemistrySelect 4 (2019) 11718–11725, https://doi.org/10.1002/slct.201902994.

[24] Z. Dikmen, O. Turhan, M. Yaman, V. Bütün, An effective fluorescent optical sensor: thiazolo-thiazole based dye exhibiting anion/cation sensitivities and acidochromism, J. Photochem. Photobiol. A Chem. 419 (2021) 113456, https://doi.org/10.1016/j.jphotochem.2021.113456.

[25] A. Khatun, D.K. Panda, N. Sayresmith, M.G. Walter, S. Saha, Thiazolothiazole-based luminescent metal-organic frameworks with ligand-to-ligand energy transfer and Hg^{2+}-sensing capabilities, Inorg. Chem. 58 (2019) 12707–12715, https://doi.org/10.1021/acs.inorgchem.9b01595.

[26] X.-C. Huang, Y. Jiang, Z. Han, W. Yong, Q. Huang, W.-X. Shi, X.-R. Chen, J.-J. Kong, H. Wu, A thiazolothiazole based Zn(II) metal−organic framework with multi-responsive fluorescent sensing toward Al^{3+} and oxoacid anions in an aqueous solution, J. Mol. Struct. 1289 (2023) 135897, https://doi.org/10.1016/j.molstruc.2023.135897.

[27] V. Kumar, S. Sony, N. Kaur, S.M. Mobin, P. Kaur, K. Singh, Thiazolothiazole based donor-π-acceptor fluorophore: protonation/deprotonation triggered molecular switch, sensing and bio-imaging applications, Anal. Chim. Acta. 1206 (2022) 339776, https://doi.org/10.1016/j.aca.2022.339776.

[28] S. Millan, G. Makhloufi, C. Janiak, Incorporating the thiazolo[5,4-*d*]thiazole unit into a coordination polymer with interdigitated structure, Crystals 8 (2018) 30, https://doi.org/10.3390/cryst8010030.

[29] J.A. Zampese, F.R. Keene, P.J. Steel, Diastereoisomeric dinuclear ruthenium complexes of 2,5-di(2-pyridyl)thiazolo[5,4-*d*]thiazole, Dalt. Trans. 9 (2004) 4124, https://doi.org/10.1039/b412344a.

[30] J.W. Slater, P.J. Steel, Syntheses of new binucleating heterocyclic ligands, Tetrahedron Lett. 47 (2006) 6941–6943, https://doi.org/10.1016/j.tetlet.2006.07.132.

[31] A.F.R. Cerqueira, M.G.P.M.S. Neves, A. Jorge Parola, A.C. Tomé, Pyridin-2-ylthiazolothiazoles – synthesis and photophysical properties, Results Chem. 3 (2021) 100246, https://doi.org/10.1016/j.rechem.2021.100246.

[32] J.E. Beves, J.J. Danon, D.A. Leigh, J.-F. Lemonnier, I.J. Vitorica-Yrezabal, A solomon link through an interwoven molecular grid, Angew. Chemie Int. Ed. 54 (2015) 7555–7559, https://doi.org/10.1002/anie.201502095.

[33] J.J. Danon, D.A. Leigh, S. Pisano, A. Valero, I.J. Vitorica-Yrezabal, A six-crossing doubly interlocked [2]catenane with twisted rings, and a molecular granny knot, Angew. Chemie Int. Ed. 57 (2018) 13833–13837, https://doi.org/10.1002/anie.201807135.

[34] D.P. August, R.A.W. Dryfe, S.J. Haigh, P.R.C. Kent, D.A. Leigh, J.-F. Lemonnier, Z. Li, C.A. Muryn, L.I. Palmer, Y. Song, G.F.S. Whitehead, R.J. Young, Self-assembly of a layered two-dimensional molecularly woven fabric, Nature 588 (2020) 429–435, https://doi.org/10.1038/s41586-020-3019-9.

[35] D.A. Leigh, J.J. Danon, S.D.P. Fielden, J.-F. Lemonnier, G.F.S. Whitehead, S. L. Woltering, A molecular endless (74) knot, Nat. Chem. 13 (2021) 117–122, https://doi.org/10.1038/s41557-020-00594-x.

[36] A. Patil, S. Salunke-Gawali, Overview of the chemosensor ligands used for selective detection of anions and metal ions (Zn^{2+}, Cu^{2}+, Ni^{2+}, Co^{2+}, Fe^{2+}, Hg^{2+}), Inorganica Chim. Acta. 482 (2018) 99–112, https://doi.org/10.1016/j.ica.2018.05.026.

[37] M.R. Pinto, Y. Takahata, T.D.Z. Atvars, Photophysical properties of 2,5-diphenyl-thiazolo[5,4-*d*]thiazole, J. Photochem. Photobiol. A Chem. 143 (2001) 119–127, https://doi.org/10.1016/S1010-6030(01)00520-2.

[38] P.K. Mandal, J.S. McMurray, Pd−C-induced catalytic transfer hydrogenation with triethylsilane, J. Org. Chem. 72 (2007) 6599–6601, https://doi.org/10.1021/jo0706123.

[39] B. Valeur, M.N. Berberan-Santos, Molecular Fluorescence, Wiley-VCH Verlag GmbH & Co. KGaA, Weinheim, Germany, 2012. https://doi.org/10.1002/9783527650002.

[40] R. Singh, G. Das, Fluorogenic detection of Hg^{2+} and Ag^{+} ions via two mechanistically discrete signal genres: a paradigm of differentially responsive metal ion sensing, Sensors Actuators, B Chem. 258 (2018) 478–483, https://doi.org/10.1016/j.snb.2017.11.097.